International Journal of Heat and Technology
Vol. 44, No. 2, April, 2026, pp. 576-590
Journal homepage: http://iieta.org/journals/ijht

# Experimental and Theoretical Study Based on Artificial Neural Networks of Photovoltaic Thermal Collector Using Air Cooling Through a Hybrid Solar Chimney

Ayat Ahmed*, Khalid F. Sultan

Department of Electromechanical Engineering, University of Technology, Baghdad 10066, Iraq

Corresponding Author Email: Eme.22.37@grad.uotechnology.edu.iq

Copyright: ©2026 The authors. This article is published by IIETA and is licensed under the CC BY 4.0 license (http://creativecommons.org/licenses/by/4.0/).

https://doi.org/10.18280/ijht.440212

**Received:** 19 December 2025
**Revised:** 5 March 2026
**Accepted:** 17 March 2026
**Available online:** 30 April 2026

***Keywords:***
*photovoltaic/thermal, hybrid solar chimney, Artificial Neural Network, air cooling, electrical efficiency, thermal efficiency*

**ABSTRACT**

Global warming represents a significant global challenge, emphasizing the urgent need for sustainable and environmentally friendly energy generation systems based on renewable resources. In this study, the performance of a hybrid photovoltaic/thermal (PV/T) system integrated with a solar chimney (SC) was experimentally evaluated to address the reduction in electrical efficiency caused by elevated photovoltaic (PV) module temperatures. Monocrystalline PV collectors were tested under varying operating conditions to assess power output and overall system performance. The results indicated that incorporating the SC notably enhanced airflow and ventilation, leading to a reduction in module temperature by approximately 5–13 ℃ compared to a conventional PV/T system. This reduction in temperature alleviated thermal stress on the solar cells and resulted in a significant improvement in electrical efficiency, which reached a maximum value of 15.8% at the highest airflow rate of 0.191 kg/s. Additionally, an Artificial Neural Network (ANN) model was developed and trained using experimental data to analyze the system's dynamic behavior. Key operating parameters, such as airflow rate, solar irradiance, ambient temperature, and cell temperature, were considered in the model. The model predictions showed strong agreement with experimental measurements, achieving high accuracy in estimating electrical and thermal efficiencies with minimal deviation. These results confirm that integrating SCs with PV/T systems, supported by Artificial Intelligence (AI) techniques, offers a practical and effective approach to improving system performance and reliability, particularly in hot climates. Furthermore, this approach lays the groundwork for various applications, including solar-assisted cooling, agricultural drying, and the enhancement of electricity generation efficiency. These advantages further support the potential of such systems as a sustainable and reliable component of future energy strategies.

## 1. INTRODUCTION

The growing global demand for sustainable energy solutions has led to increased interest in hybrid systems that combine photovoltaic (PV) and thermal (T) energy recovery. The performance of such systems, however, is often limited by high temperatures, which reduce both electrical and thermal efficiencies. Solar chimneys (SCs), widely recognized for their ability to enhance airflow and cooling, offer a promising solution to mitigate this issue. Recent studies have optimized various parameters of SCs, such as chimney height, tilt angle, and air gap, to improve thermal performance and enhance energy recovery. Despite these advances, there remains a significant gap in research focusing on the integration of SCs with hybrid photovoltaic/thermal (PV/T) systems to enhance their electrical and thermal performance [1, 2]. How to meet the ever-increasing needs and wants in an environmentally sustainable manner has become one of the major issues to be addressed by contemporary societies [3]. Traditional Carbon-Based energy harvesting methods have been instrumental in economic growth, but the upcoming challenges of resource depletion, environmental pollution, and climate change questions on-going use of these resources [4]. The evolution of industrial development in modern economies is profoundly influenced by the adequacy and efficiency of their energy supply systems. Their energy usage influences people's standard of living [5]. There are many purposes for which we need energy, such as transport, agriculture, industries, lighting, and all the home appliances we use. It is estimated that fossil fuels were used to produce electricity before the Industrial Revolution [6]. The unsustainable depletion of conventional fossil energy resources at an accelerated pace has resulted in a serious “energy crisis” and the deterioration of environmental conditions, such as ozone layer degradation, emission of harmful greenhouse gases (GHGs) into the atmosphere, and global warming, which not only pose a hazard to human security but also to the future sustainability of Planet Earth [7]. Therefore, it is increasingly becoming important to seek clean and environmentally friendly energy sources in an effort to reduce reliance on fossil fuels and mitigate the adverse environmental effects imposed [8]. Solar power is being the most accepted and accessible renewable energy generated

which are relatively clean, abundant, sustainable and inexhaustible resources of light energy [9, 10]. PV converting systems are a growing trend for harnessing solar energy into electric power and thermal energy [11].

Figure 1 shows the operation Principles of the hybrid PV/T system and configurations where both electrical and thermal conversion are operated in sequence to enhance the energy transformation/efficiency. In the first place, PV panels absorb solar radiation and transform a part of this solar energy into electric power. During the conversion, surplus heat is released as waste and stored in the PV cells, causing an increase in the temperature of operation. To reduce this thermal heating, a cooling system is used to dissipate the excess heat from the PV module. Thus, the recovered thermal energy is further used for beneficial heating purposes such as space heating, drying, or hot water supply. Additionally, by properly utilising and recycling the produced heat, system efficiency is improved. This coupled cycle illustrates that the combined use of electrical and thermal energy simultaneously results in enhanced performance and sustainability of PV/T systems. Magnetocaloric coupling, as opposed to traditional engines, based on a thermodynamic fermion particle model, 18 one can instead exploit magnetocaloric.

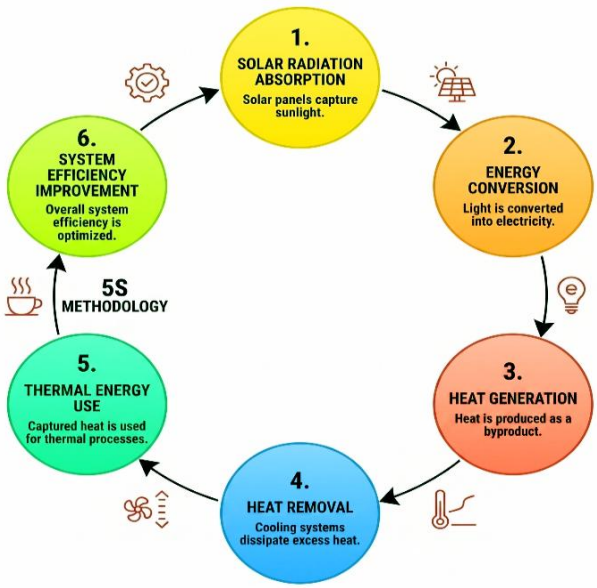


**Figure 1.** Schematic illustration of the energy conversion and heat recovery cycle in a hybrid photovoltaic/thermal (PV/T) system

While several studies have explored the role of Computational Fluid Dynamics (CFD) and experimental methods in optimizing SC designs, Artificial Intelligence (AI) models, particularly Artificial Neural Networks (ANNs), have not been adequately applied to predict and optimize the performance of hybrid PV/T-SC systems. This gap in research highlights the need for more sophisticated, data-driven models that can simulate real-world conditions and optimize system performance under varying operational parameters. By integrating ANN-based performance prediction with experimental validation, this study aims to address the limitations of traditional methods, offering a novel approach to improving energy recovery, efficiency, and economic viability of hybrid systems, particularly in hot and arid climates.

Solar PV systems produce electricity by directly transforming part of the incident solar radiation into electrical power, and the common conversion efficiencies are between 19% and 21% [12]. The rest of the incoming energy of the sun is reflected either at the surface of the module or the PV cells, which absorb the heat. This heating causes the temperature of the cell to rise, which negatively impacts the electric performance of the PV module. The most common operational issue in PV systems is overheating, especially in areas with large solar irradiance and high ambient temperatures, where excessive heating causes conversion efficiency to decline dramatically [13]. In order to deal with this problem, various cooling and thermal control methods have been suggested and researched over the last few years. One such technology has been PV/T systems, whereby a cooling system is utilized to complement the PV module in order to remove the excess heat. The PV/T system is a setup where a working fluid, liquid or gas, is circulated behind or underneath the PV panel, enabling the system to both produce electrical power and provide useful thermal energy in a single integrated unit. The result of this two-energy production is the improvement of the total efficiency and use of solar energy. PV/T hybrid system is a typical set comprising a PV module and a heat extraction device. Even though the PV module receives almost 80 percent of all the incident solar radiation, not all the energy received is converted into electricity, which is determined by the conversion efficiency of the cells. The rest of this absorbed energy is lost as heat, and this heat can be considered as an output of the PV/T system because it can be removed and used efficiently to reduce the temperature level of the cells and provide an overall better performance of the system [14].

In another CFD analysis is carried out on thermal performances of a flat plate solar collector for various numbers of air inlets [15]. The obtained results reveal that a three-inlet type possesses the maximum value of exit temperature, then two- and on single- inlets, all having higher exit temperatures than those for two and one-inlet designs. In addition, as the heat flux increases and/or the inlet velocity decreases, the exit air temperature increases. Using an underground heat exchanger, the air was precluded in another research work [16]. This study carried out tests to investigate the influence of flow rates and hot ambient air temperatures in the range of 35 ℃, 40 ℃, and 45 ℃ on module efficiency. An effective heat exchanger was demonstrated to maintain the appropriate temperature, and using this cooling method can increase the daily electricity efficiency up to 29.11% [17].

The thermal performance of SCs was presented in a building built with local stones and hollow bricks on the roof. It was found that slope angle, building material selection, and air gap were important to the performance. The optimum chimney parameter was 1 m × 0.65 m(s), with an air gap of 0.25 true and an inclination angle of 45°, giving respective ACH values at solar intensities of approximately 5, 6.5, and 7.8 ACH [18]. Performance enhancement of SCPP by tuning collector tilt angle and chimney designs has been investigated. ANSYS-FLUENT simulation results revealed that the 50% tilt of the collector enhanced the air velocity by 12% and P tapered by 23% higher than that with full tilt. The performance was also better for the semi-divergent chimney coupled with a fully tilted collector, where the average air temperature increase reached 17 K. These results indicate that the correction of collector angle and design of chimney system are vital in improving thermal efficiency of SCPP [19].

Previous studies have shown that SC performance can be significantly improved through the careful optimization of

geometric and operational parameters such as chimney height, tilt angle, air gap, thickness, and width. Key factors, including chimney width, air gap, and inclination angle, have been identified as crucial elements influencing airflow and thermal comfort. Building upon these findings, the present study introduces a highly innovative hybrid PV/T system integrated with a SC, combined with ANN modeling for performance prediction and optimization. Unlike traditional approaches that rely solely on CFD simulations or experimental optimization, this study integrates both experimental investigation and ANN-based performance prediction, offering an advanced solution for simulating and optimizing the system under real-world operating conditions. This novel coupling of ANN modeling with physical system enhancement represents a cutting-edge approach to simultaneously improve both electrical power generation and thermal energy recovery, overcoming the operational limitations of conventional solar collectors, particularly in extreme high-temperature environments. The proposed hybrid system significantly expands the potential applications of PV/T-SC technologies, particularly in hot and arid climates, enhancing the economic viability of these systems in solar-assisted cooling, space heating, agricultural drying, and domestic hot water production.

## 2. THE EXPERIMENTAL CONFIGURATION AND METHODS

### 2.1 Photovoltaic module selection and characteristics

It is crucial to have an unambiguous experimental setup in evaluating the thermal and electrical performance of PV/T systems. The type of PV module, material layers, geometry dimensions, and thermal insulation are key points to characterize the efficiency and reliability of the system. Special attention was given to choosing a PV module and structural configuration for the hot climatic conditions. The number of cells, cell size, efficiency of a conversion and physical dimensions of a module are the most important parameters to be considered when choosing a PV panel. In this study, a monocrystalline PV panel was adopted owing to its high conversion efficiency, long lifetime and good performance under high solar radiation. The chosen module has an average conversion efficiency equal to 22% according to manufacturer's data are presented in Table 1.

Figure 2 depicts the multi-layered structure of the silicon PV module used in this study. Every solar cell is encapsulated with a special high-strength tempered glass to protect it from the extreme environment. The panel can withstand high wind (2400 Pa) and snow loads (5400 Pa), a lightweight anodized aluminium frame and reinforced Safety and anti-Reflection coated glass 3. The module's front surface is made of glass, which gives the maximum transmittance and protects cells from the environment. The rear substrate of the PV module is typically made of Tedlar, a tough polymer that provides a moisture barrier as well as being highly resistant to UV-light, mechanical stress, and weathering. These material characteristics greatly contribute to the overall long-term development and stability of the PV module, so that one can count on an operational period ranging from 25 years or even more when considering normal operation conditions [20]. The particular system configuration, along with the careful thermal and structural design considerations, offers a robust experimental platform to evaluate the integration of PV/T collectors with SC.

**Table 1.** Specifications of a mono-crystalline photovoltaic (PV) panel

| Parameter | Value |
|---|---|
| Type of PV module | TYM-130W |
| Dimensions (mm) | 1480 × 680 × 35 |
| Maximum power (Pmax) | 130W |
| Short circuit current (Isc) | 8.09A |
| Open circuit voltage (Voc) | 21.24 V |
| Voltage at maximum power (Vmp) | 18.0 V |
| Current at maximum power (Imp) | 7.22 A |

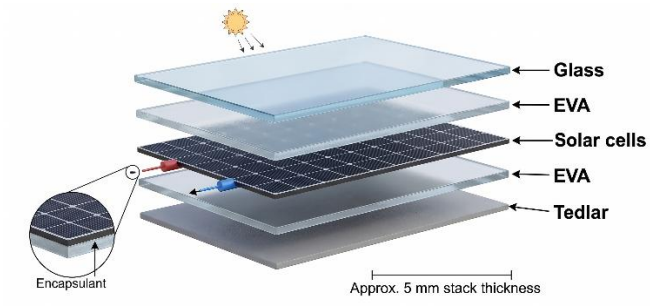


**Figure 2.** Photovoltaic (PV) module layers (Glass to Tedlar type)

### 2.2 Photovoltaic/thermal collector and solar chimney configuration

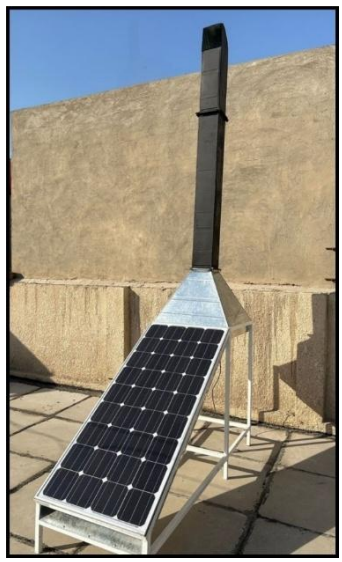

**Figure 3.** Photovoltaic/thermal (PV/T) System with solar chimney (SC)

The experimental system layout is illustrated in Figure 3. A TYM-130W monocrystalline solar panel was mounted on a steel frame, and the outdoor performance of the system was evaluated under various Iraqi climatic conditions. Based on the geographic coordinates of Baghdad Governorate, the solar absorption section was oriented south at a 33.3-degree tilt angle to optimize solar energy absorption. To facilitate airflow, a rectangular aluminum passage was created behind the panel, measuring 148 cm long, 68 cm wide, and 7 cm deep. Finally, the passage is provided with an air inlet at its bottom portion and an outlet at its top portion in communication with

a convergent nozzle equipped with a fan. This nozzle is attached to a vertical collector square duct. This channel, 20 cm in diameter and 2 m high, effectively serves as a chimney. Air velocity within the chimney increases with the employment of a convergent nozzle. Thermal protection from all sides was provided by a 10 mm thick foam sheet coated with a reflective layer (as shown in Figure 4) on the collector's side walls and bottom.

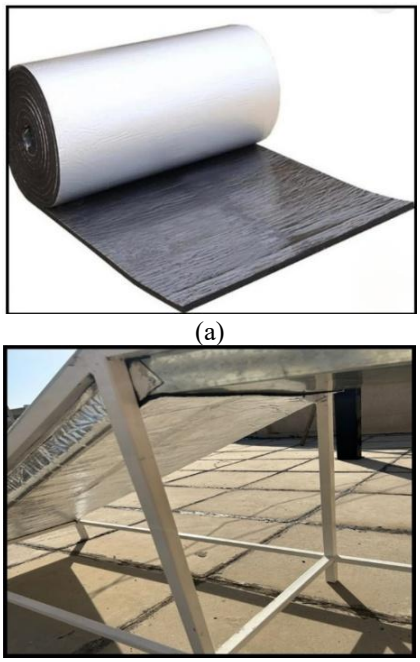

(a) (b)

**Figure 4.** (a) Foam insulation material and (b) its application beneath the photovoltaic/thermal (PV/T) collector for thermal insulation

### 2.3 Instrumentation

Reliable measurement and data collection are the key to quality assessment of the performance of PV/T systems under various operative conditions. For this reason, an array of electrical and electronic instruments was used to follow solar radiation, air fluxes and flows, generated power, and thermal data in real time, also allowing accurate control as well as experimental data recording. In this study, a solar power meter, shown in Figure 5, was used to accurately measure the intensity of solar radiation within a range of 0 to 1999.9 W/m². The photosensitive part detects the incident solar light, while the LCD display presents the measured radiation value. The unit selection key is used to change the measurement unit, and the ON/OFF and hold buttons are used to operate the device and stabilize the readings during the experiments. A 12-volt DC fan, shown in Figure 6, was used to maintain efficient cooling and ventilation within the system. The fan enhances airflow and heat dissipation by forcing air through the duct and surrounding components. In addition, a convection fan was installed at the duct inlet to improve air circulation. The fan is enclosed in a solid galvanized steel housing, which protects the internal components and directs air through the small openings between the louvered blades to ensure uniform airflow distribution and stable operating conditions. In order to measure and obtain experimental data, a dedicated electronic control unit was designed using an Arduino Mega 2560 microcontroller board, as shown in Figure 7. The control unit is responsible for monitoring, processing, and recording the system parameters during operation. It includes electronic circuits, relays, wiring connections, and sensor interfaces integrated inside a protective enclosure to ensure reliable control and data acquisition throughout the experiments. There are several sensors (such as temperature, current, voltage) works with this board through input/output modules. It is also provided with a 20 × 4 Liquid Crystal Display (LCD) for the measured value to be displayed in real time while working, and an SD card module to save measurements from time to time for later analysis. All its electronic parts are encased in a closed acrylic box to guard against rough environmental conditions and, at the same time, for easy maintenance, and reading connections are given.


**Figure 5.** The solar power meters

**Figure 6.** The fan

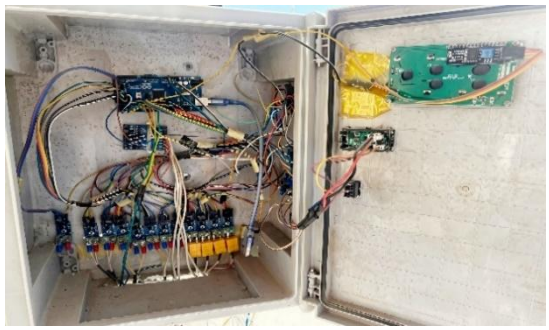

**Figure 7.** The Arduino Mega module

A compact anemometer and thermometer (model UT363/UT363BT) were used to measure the air velocity in the collector channel, as shown in Figure 8. The device can measure the air velocities up to 30 m/s and it was employed to measure the airflow conditions accurately in the course of the experiment. Air temperature and velocity were measured simultaneously to enable the accurate determination of the rate of air mass flow through the PV/T collector. A DC voltage regulator (DC VRR) was used to adjust the rotational speed of the cooling fan to control and regulate the airflow under various operating conditions by pulse width modulation (PWM) technology. The approach to control allowed controlling the rate of air mass flow into the system accurately. The voltage regulator has a maximum current output of 10 A and can work with an input voltage up to 12 V, which is why it is quite useful in the DC fans. The regulator has two major terminals, one of which is attached to the DC fan and the other to the power supply, as depicted in Figure 9. This arrangement gave the stable and reliable operation of the fans during the experimental tests, and a consistent flow of air and repeated conditions of measurement.

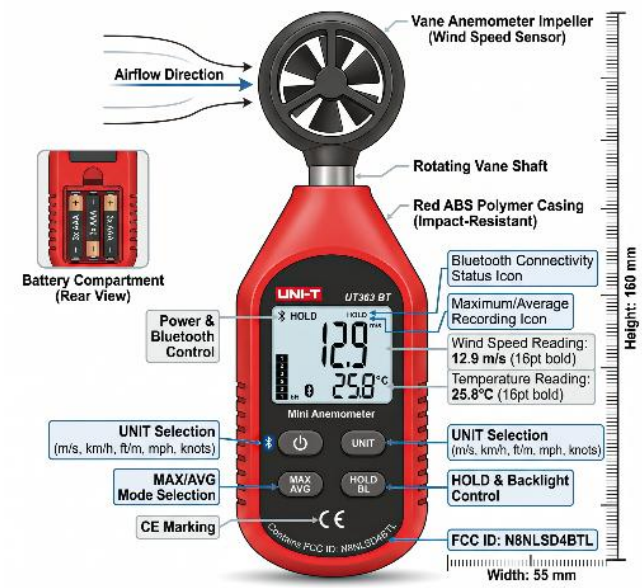


**Figure 8.** Mini anemometer device

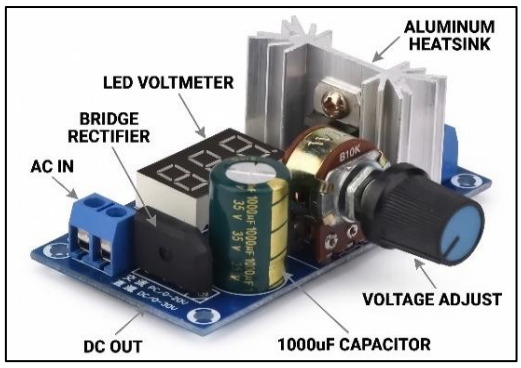


**Figure 9.** Voltage regulator

A solar-charge controller (LCD type) with 12/24 V and 30 A of functionality was used to control the input voltage and current from the PV panels to the Energy Storage System (ESS), as presented in Figure 10. The key role of this controller is to protect the battery from overcharging and deep discharging. It also offers critical defence against electrical defects like overload, short circuit, and reverse polarity easy for you to maximize system safety and reliability. The charge controller is also used to ensure that voltage fluctuations are minimized as it controls variations in solar radiation levels and load utilization, which further contributes to keeping the battery performance at its peak, allowing for an extended battery life. This control is of special importance for the dynamic operation, as it is tested in an open field. For energy storage, here lead–acid battery with a nominal rating of 12 V and 9 Ah was employed, as it has been depicted in Figure 11. These batteries collect the electric power produced by the PV plates and provide energy for the system's electrical parts when in use. Everything in the system was conceived to run on DC, making it very efficient to connect PV sources, charge control blocks, batteries, and loads in a unique DC power system.


**Figure 10.** Solar charge controller

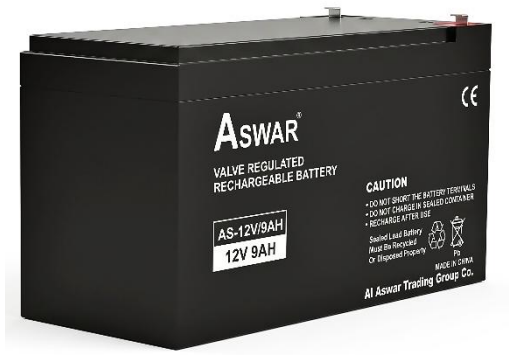


**Figure 11.** Lead-acid batteries

## 3. MODEL EQUATIONS FOR PERFORMANCE EVALUATION

The electrical and thermal efficiencies of a PV/T system are normally measured in terms of both the electrical and thermal efficiency of the system, which combined, represent the capability of the system to efficiently transform incident solar energy into useful electrical power and recoverable thermal energy. Proper evaluation of these performance indicators can be critical in the analysis of the system behavior in various operating and environmental conditions. With the help of the measurements of the current and voltage taken during the operation of the PV panel, the electrical output of the PV panel

can be calculated. It is these electrical parameters that allow the calculation of the instant power output and the electrical efficiency of the PV module [21]. Simultaneously, thermal performance is considered by examining the amount of heat that is conducted to the working fluid by the PV module, which is related to the mass flow rate, temperature difference, and specific heat capacity of the fluid [22]. The equations governing the calculation of electrical power, electrical efficiency, and thermal efficiency of the PV/T system are given in the following subsections.

$$Isc = Isc_{ref} + K_I\,(T_c - T_{c,ref}) \tag{1}$$

$$Voc = Voc_{,ref} + K_V\,(T_c - T_{c,ref}) \tag{2}$$

where, $T_c$ is the temperature of the cell $Isc$ represents the short-circuit current, $Voc$ stands for the open-circuit voltage, $K_I$ and $K_V$ the temperature coefficients for voltage and current, respectively.

$$P = Isc \times Voc \times FF \tag{3}$$

where, $FF$ denotes the fill factor, which is assumed to be 0.75. The PV/T module's overall, thermal, and electrical efficiency can be evaluated according to [23]:

$$\eta_{\text{ele}} = \frac{P}{G \times A} \tag{4}$$

$G$ denotes the incident solar irradiance on the module in units of watts per square meter (W/m²), while A represents the module's area (m²).

The equation can calculate the module efficiency suggested by [22].

$$\eta_m = \eta_c \times PF \tag{5}$$

The maximum power output is obtained based on the approach reported in [23]:

$$\eta_c = \frac{P_{max}}{P_{in}} = \frac{I_{max} V_{max}}{A_c \cdot G} \tag{6}$$

where, $I_{max}$ is the maximum current, and $V_{max}$ is the maximum voltage.

The electrical effectiveness of a PV module can be calculated [24].

$$\eta_{ele} = \eta_m\left[1 - \beta\left(T_C - T_{C,ref}\right)\right] \tag{7}$$

where, $\beta$ is the Silicon temperature coefficient, which is 0.0045 1/°C, $T_{C,ref}$ is the temperature of the cell at 25 °C.

The air's mass flow rate can be computed according to [25]

$$m^{\circ}_{air} = \rho_{air} V_{air}\, A_c \tag{8}$$

The convective heat transfer to the air is obtained following the approach reported in [26]:

$$Q_{conv} = m^{\circ}_{air}\, Cp_{air}\left(T_{o,air} - T_a\right) \tag{9}$$

The flow rate, specific heat, intake, air exit temperatures, and solar irradiation are all factors that affect thermal efficiency. In a steady-state setting, it is provided according to [27]:

$$\eta_{th} = \frac{Q_{conv}}{A_C I_t} \tag{10}$$

## 4. ARTIFICIAL NEURAL NETWORK

ANN models are advanced computational architectures that mimic aspects of human cognition, such as those related to knowledge representation, prediction, and categorization. Unlike the traditional programs, ANNs are developed to learn and recognize patterns in data with training on datasets. Layer-wise connected input, hidden, and output neurons are used in these models, as shown in Figure 12, where they have to decide on progressively incoming and processing responses. There are weighted connections between the neurons, and the neuron-outputs influenced by a transfer function. The performance of ANNs can be improved through a training process, which is normally conducted iteratively based on a gradient descent approach in an attempt to minimize errors by adapting weights. Backpropagation, a gradient descent procedure that is most widely used, is significantly prevalent, but it is also often the case that finding a good training strategy for good training success in a given task necessitates a rather ad-hoc approach [28].

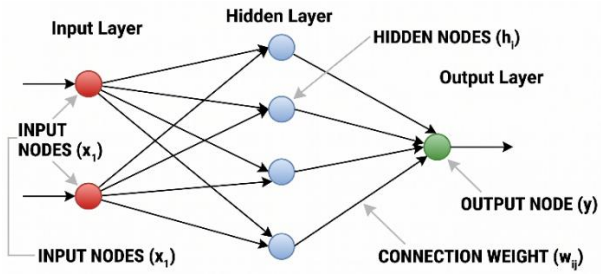


**Figure 12.** Structure of the Artificial Neural Network (ANN)

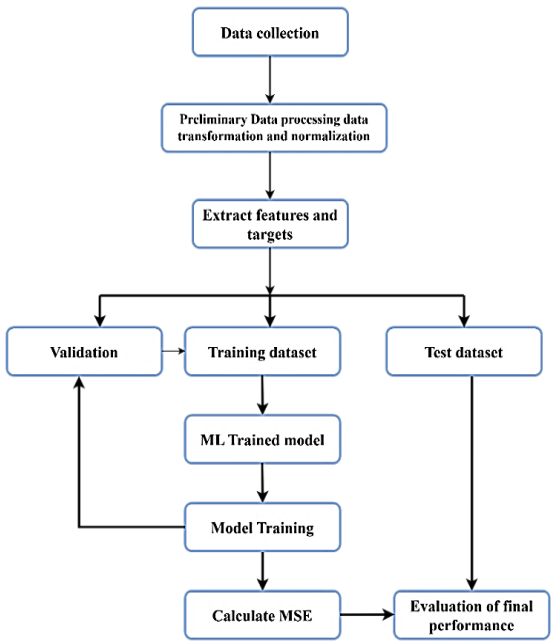


**Figure 13.** Flowchart of Artificial Neural Network (ANN) data processing and evaluation

### 4.1 Artificial Neural Network methodology

The ANN model was trained using the backpropagation algorithm with the Levenberg-Marquardt optimization method. The ANN framework implemented in this study was based on a structured learning process that included experimental data collection, pre-processing, variable extraction, model construction and training, and performance evaluation. Figure 13 illustrates the complete workflow of the ANN model development methodology adopted in this study.

### 4.2 Development of the Artificial Neural Network model for hybrid photovoltaic/thermal - solar chimney system

ANNs were employed in this study as an advanced modelling tool to simulate and predict the performance of the hybrid PV/T system integrated with an SC. The use of ANN techniques enables accurate representation of the complex and nonlinear relationships between environmental conditions, operating parameters, and system performance. Based on the available experimental data, three distinct ANN-based predictive models were developed to evaluate the electrical, thermal, and aerodynamic behaviour of the hybrid system.

1) **Electrical and Thermal Efficiency Model:** This model was developed to predict the electrical efficiency of the PV panel and the thermal efficiency of the PV/T system. It utilizes five input variables, including ambient air temperature, PV panel voltage, PV panel current, solar irradiance, and PV cell temperature. These parameters were selected due to their direct influence on both electrical power generation and heat recovery performance.
2) **SC Outlet Temperature Model:** The second ANN model was designed to estimate the outlet air temperature of the SC. The model incorporates five input parameters: inlet air temperature, absorber surface temperatures at multiple locations, ambient air temperature, and solar irradiance. This model provides insight into the thermal behavior of the SC and its contribution to airflow enhancement and heat extraction.
3) **PV Module Temperature Model:** The third ANN model focuses on predicting the operating temperature of the PV module. It considers several influential variables, including the temperature of the back surface of the module, wind speed, solar irradiance, relative humidity, inlet air temperature, and ambient air temperature. Accurate prediction of module temperature is essential, as it strongly affects electrical efficiency and long-term module reliability.

The development of these ANN models allows a comprehensive assessment of the hybrid PV/T–SC system and provides a reliable tool for performance prediction under varying climatic and operational conditions.

### 4.3 Configuration and training of the Artificial Neural Network model

The development and implementation of ANN model were done with the help of MATLAB software (R2019a). The network architecture was set up in accordance with the chosen input and output parameters, and preliminary weight values were set in the network before the training process. In training, input data was presented to the network in small steps, and output predictions were made, which were compared to respective target (experimental) values constantly. The training was conducted in the form of an iteration-based supervised learning strategy. The network changes its weight matrices after each iteration to reduce the prediction error. The training was stopped when the network output converged enough to the desired output values, and the Mean Square Error (MSE) was at an acceptable predetermined threshold. In case convergence was not attained, then the training process was repeated with different weight values until good performance was realized. In order to test the predictive ability of the ANN model, the network outputs were compared with the analytical and experimental data that were obtained under Baghdad climatic conditions. A number of ANN architectures with varying numbers of input neurons and hidden-layer neurons have been studied to establish the best network topology that gives high accuracy without over-fitting. The measures of standard statistical features such as the coefficient of determination ($R^2$), Root Mean Square Error (RMSE), and coefficient of variation (COV) were used to assess the performance of every ANN configuration as explained in the following Eqs. (11)–(13) [29]. The accuracy, reliability, and generalization ability of the developed ANN models were evaluated by these metrics.

$$RMSE = \sqrt{\frac{1}{n_s}\sum_{i=1}^{n_s}(X_i - Y_i)^2} \tag{11}$$

$$R^2 = 1 - \left[\frac{\sum_{I=1}^{ns}(X_i - Y_i)}{\sum_{i=1}^{n_s} X_i}\right] \tag{12}$$

$$COV = \frac{RMSE}{\sum_{i=1}^{n_s} X_i} * 100 \tag{13}$$

where, *Ns* is the number of data measured in the experimental study, and refers to the experimental and simulated data, respectively.

When RMSE and COV are minimized (approach 0) and R (or $R^2$) approaches 1, it indicates the network performances are excellent. ANNs are composed of an input layer, an output layer and one or more hidden layers. Each layer comprises interconnected neurons. The output of each layer is the input to the next, passed through a transfer function (activation). In this study, the Tangent Sigmoid is used as an activation function in the neural networks because it has an output distribution that is much more centered around zero, leading to a faster learning speed and larger gradients than those generated using the Sigmoid. This addresses the vanishing gradient problem and enhances the experimental performance of the network [30].

$$\tan(x_i) = \frac{e^{xi} - e^{-xi}}{e^{xi} + e^{-xi}} \tag{14}$$

The input data are normalized to the interval [0, 1] to be suitable for the activation function.

## 5. RESULTS AND DISCUSSIONS

This section presents and discusses the experimental and analytical results obtained from the hybrid PV/T system

integrated with an SC. The system was operated under forced air-cooling conditions at three different air mass flow rates, namely 0.0635, 0.127, and 0.191 kg/s, in order to evaluate the influence of airflow on thermal regulation and electrical performance.

For each operating condition, the electrical characteristics of the PV module were monitored by measuring the output voltage and current throughout the test period. These measurements were used to calculate the maximum power output and electrical efficiency of the system using Eqs. (6) and (7). The comparative analysis of the three airflow conditions allows assessment of the effectiveness of the SC–assisted cooling mechanism and its impact on both electrical and thermal performance. The following subsections detail the weather conditions, experimental observations, and ANN-based analytical results, providing a comprehensive discussion of system behavior under varying operating and environmental parameters.

### 5.1 Weather data

The meteorological data obtained in June 2025 were discussed and demonstrated as mean values within the daily working period 7:00 AM to 5:00 PM. The parameters that have been monitored are the solar irradiance and ambient temperature, which are important factors that dictate the performance of the PV/T system. The findings (as shown in Figure 14) reveal that the solar irradiance continued to rise gradually during the morning hours and reached its highest average of about 1100 W/m$^2$ at about 2:00 PM. Following this irradiance peak, the irradiance slowly declined towards the late afternoon. Such climatic conditions offered a representative and appropriate data set to test the performance of the system with high levels of solar radiation, which is common during summer seasons in Baghdad.

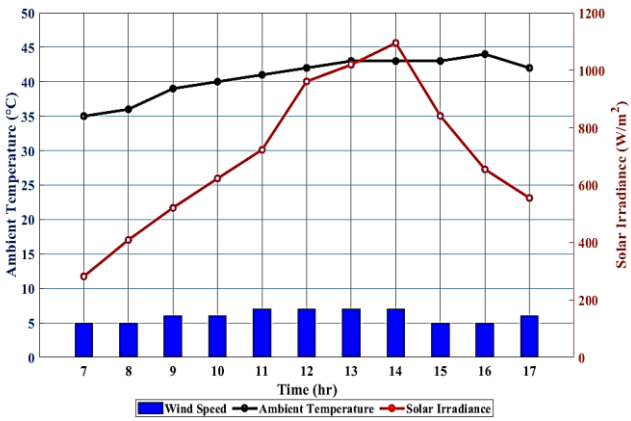


**Figure 14.** Hourly profiles of solar irradiance, ambient temperature, and wind speed recorded during the experimental period (07:00–17:00)

### 5.2 Experimental results

High temperature conditions of PV cells are a significant negative influence on both the electrical capabilities and the overall efficiency of PV panels. As the temperature of PV cells increases, their efficiency decreases, leading to lower power output. This phenomenon is particularly prominent in regions with high solar irradiance and elevated ambient temperatures, where the thermal stress on PV cells becomes more pronounced. To overcome this issue, air was used as the cooling medium in this experiment. This section investigates how varying the rate of air mass flow can be utilized to reduce the temperature of the PV modules and enhance the performance of the system.

Three different air mass flow rates were tested: 0.0635 kg/s, 0.127 kg/s, and 0.191 kg/s. These values were selected to evaluate the effectiveness of air cooling in reducing the temperature of the PV cells and controlling the outlet air temperature. Additionally, the electrical and thermal performances of the PV/T system were compared to identify the most effective cooling approach.

Figure 15 illustrates how the temperature of the PV module changes throughout the day under varying airflow conditions. Without an active cooling system, the maximum temperature of the PV cells reached approximately 68 ℃ during midday. However, when the air-cooling system was activated, a significant drop in module temperature was recorded across all three mass flow rates. The maximum temperatures of the cells were found to be 65 ℃, 58 ℃, and 55 ℃ at the air mass flow rates of 0.0635 kg/s, 0.127 kg/s, and 0.191 kg/s, respectively.

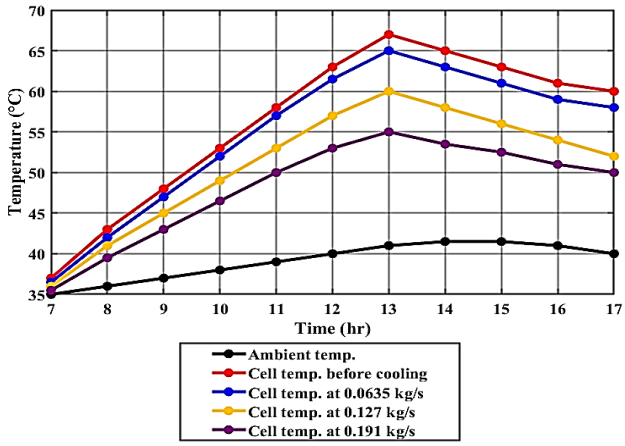


**Figure 15.** Cell temperature variations with different air mass flow rates

These results demonstrate that increasing the air mass flow rate improves the heat dissipation rate of the PV module, leading to better thermal control and lower operating temperatures. This improved cooling efficiency reduces the thermal stress on the PV cells and prevents performance degradation, allowing the system to operate at its optimal capacity.

The observed reduction in temperature can be attributed to convective heat transfer, where the air flow removes excess heat from the PV module. As the air mass flow rate increases, the convective heat transfer coefficient (h) increases, enhancing the cooling efficiency. This mechanism results in lower PV cell temperatures, which in turn improves the overall electrical performance of the system. The chimney effect further enhances this cooling process, as the vertical air duct generates a pressure difference, which accelerates the airflow, improving heat extraction from the PV cells.

Figures 16 and 17 illustrate the effect of varying air mass flow rates on the electrical characteristics of the PV modules, specifically focusing on output power and electrical efficiency. The results demonstrate a clear correlation between increased airflow and improved electrical performance. As the air mass flow rate increases, the cooling of the PV module surface is enhanced, leading to a significant rise in electrical power output.

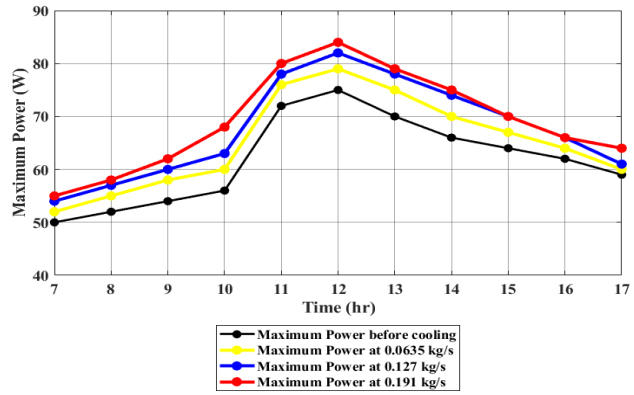


**Figure 16.** Variation of the power maximum

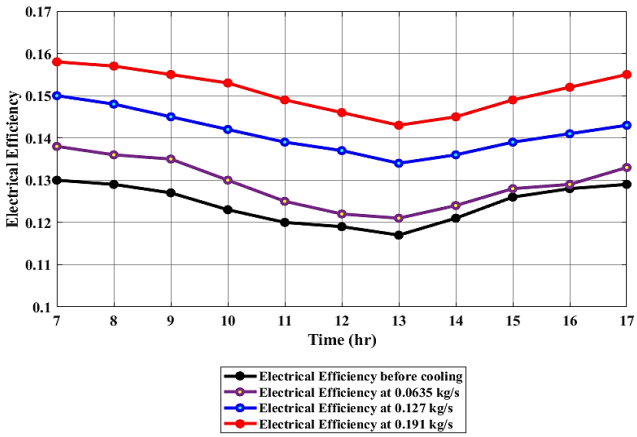


**Figure 17.** Electrical efficiency of the photovoltaic/thermal (PV/T) system

At the lowest air mass flow rate of 0.0635 kg/s, the maximum measured electrical power output was 83.5 W. As the airflow rate increased to 0.191 kg/s, the power output significantly improved, reaching a higher value due to more efficient cooling. This enhancement in power output can be attributed to the improved convective heat transfer provided by the increased airflow. The higher airflow rates facilitate the dissipation of excess heat from the PV cells, thereby reducing their operating temperature.

Likewise, the electrical efficiency of the system showed a similar upward trend with the increased airflow rate. In the uncooled scenario, the electrical efficiency was approximately 13%. However, as air cooling was applied, the efficiency gradually increased, reaching a maximum value of 15.8% at the highest air mass flow rate of 0.191 kg/s, especially during the early morning hours when the system is subjected to lower ambient temperatures and more direct sunlight.

These findings underline the importance of convective heat transfer in the cooling process. As the airflow rate increases, the rate of convective heat loss from the surface of the PV cells improves. This enhanced heat dissipation leads to a reduction in the thermal load on the PV cells, effectively lowering their operating temperature. Since PV module electrical efficiency is directly proportional to cell temperature, the decrease in operating temperature results in an increase in both electrical power output and efficiency.

The improvements in power output and efficiency underscore the effectiveness of airflow-assisted cooling in optimizing the performance of PV systems, particularly under conditions of high solar irradiance and elevated ambient temperatures. The reduced thermal stress on the PV modules allows for sustained high-performance operation, thereby proving the significant benefits of enhanced convective cooling in PV systems

PV/T systems integrated with SCs contribute significantly to improving system performance by enhancing waste heat recovery and facilitating cooling through air circulation. The temperature differences between the inlet and outlet of the SC under various air mass flow rates are shown in Figure 18. These results reveal the substantial impact that air mass flow rate has on the temperature difference across the SC.

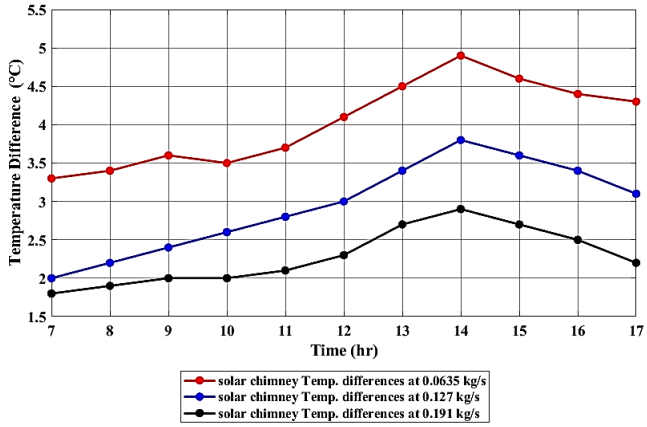


**Figure 18.** Effect of varying mass flow rates on the temperature differences in the solar chimney (SC)

At the lowest air mass flow rate (0.0635 kg/s), the temperature difference between the inlet and outlet of the chimney increases, reaching a value of 4.8 °C. This is primarily due to the longer residence time of air within the duct, which allows more heat to be absorbed by the air as it flows past the PV/T module. With more time in contact with the heated surface of the module, the air has a greater opportunity to absorb thermal energy, resulting in a larger temperature gradient between the inlet and outlet of the chimney.

On the other hand, at the highest air mass flow rate (0.191 kg/s), the temperature difference decreases to 2.9 °C. This reduction is attributed to the higher air velocity that results from increased airflow. As air moves faster, it spends less time in contact with the PV module, reducing the time available for heat absorption. Despite the faster airspeed, the higher flow rate promotes better overall heat transfer, but the rate of temperature change is less pronounced due to the shorter interaction time between the air and the heat source.

In contrast, lower air flow rates tend to lead to a greater temperature difference, as less air is moved through the system, giving it more time to absorb heat. Conversely, higher flow rates do not achieve the same temperature gradient past the heat source but lead to more effective overall heat transfer across the system. This dynamic illustrates that the balance between airflow rate and temperature difference is crucial for optimizing the thermal performance of the PV/T-SC system.

The observed trade-off between flow rate and temperature difference underscores the importance of optimizing air mass flow rates to achieve the best performance. While higher flow rates reduce the temperature difference, they increase the overall heat transfer efficiency, which may be more beneficial for maintaining lower operating temperatures in the PV cells and improving system performance over extended periods.

Thus, flow rate optimization is key to maximizing both thermal recovery and cooling efficiency in hybrid PV/T systems.

Figure 19 illustrates the effect of air mass flow rate on the thermal efficiency of the PV/T system. At the lowest air mass flow rate of 0.0635 kg/s, the thermal efficiency was relatively low, ranging between 30% and 50% during the operating period. This lower efficiency can be attributed to the reduced convective heat transfer at lower flow rates, where the air has less time to absorb heat from the PV module, leading to a higher operating temperature for the cells and, consequently, lower thermal performance.

As the air mass flow rate increased to 0.127 kg/s, there was a significant enhancement in the thermal performance of the system, with the thermal efficiency rising to approximately 54%. This increase in efficiency can be explained by the improvement in convective heat transfer. With moderate airflow, the heat extraction from the PV module is more effective, as the air moves faster, reducing the temperature gradient between the module surface and the ambient air, allowing more heat to be transferred out of the system.

The maximum thermal efficiency of approximately 57% was achieved at the highest airflow rate of 0.191 kg/s around 1:00 PM. At this point, the air velocity was sufficient to maximize heat dissipation, and the system's cooling capacity was optimized, leading to the highest recorded thermal efficiency. This improvement can be attributed to the enhanced convective heat transfer between the PV module and the airflow, which accelerates the removal of excess heat, thereby reducing the operating temperature of the PV cells.

In general, the results clearly indicate that an increase in air mass flow rate leads to improved thermal efficiency. The gradual rise in thermal efficiency with increasing airflow supports the notion that airflow optimization is crucial for enhancing the thermal performance of PV/T systems, especially those integrated with SCs. Efficient airflow helps balance the thermal load on the system, optimizing the overall performance by extracting excess heat from the PV cells and ensuring that the system operates at lower temperatures for better efficiency.

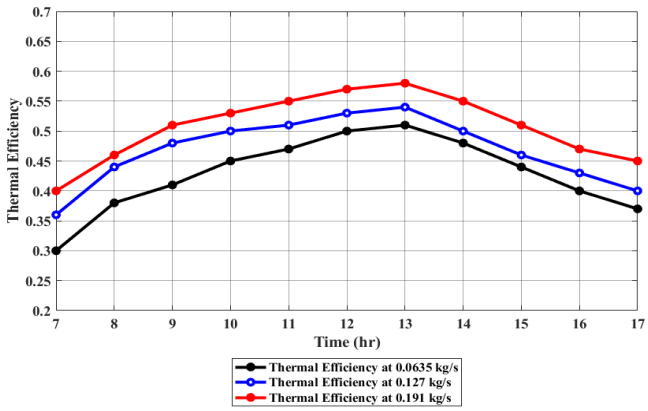


**Figure 19.** Thermal efficiency of the system

### 5.3 Analytical results of Artificial Neural Network

The present approach involves training an ANN model to optimize network weights based on the experimental data obtained from the system. The model is trained using a dataset collected over a period of one month in Baghdad, where key meteorological conditions—including ambient temperature, solar radiation, and relative humidity—were continuously monitored. This data serves as the foundation for tuning the ANN model, allowing it to learn and adapt to the environmental factors that affect system performance.

In addition to meteorological data, electrical and thermal measurements were also conducted throughout the testing period. These measurements included voltage, current, and PV cell temperature, which were recorded under a wide range of operating conditions. The data collected during the experiment were crucial for understanding the relationship between solar irradiance, ambient temperature, and the operational efficiency of the PV/T system. These measurements were then used to train the ANN model, enabling it to predict the system's performance under various environmental conditions and optimize its operation for maximum efficiency.

#### 5.3.1 Experimental and Artificial Neural Network model results for photovoltaic module temperature

A comparative analysis of the converged ANN prediction models is presented in Table 2, which includes a detailed evaluation of the convergence time per training epoch and the fitting behavior of the models to both the training and testing datasets. This comparison was conducted to assess the precision and robustness of different ANN structures in predicting the temperature of the PV module. To determine the appropriateness and validity of each model, the measured and predicted PV module temperatures were compared using several common performance indices, including:

- Mean Bias Error (MBE)
- RMSE
- Mean Percentage Error (MPE)
- Correlation Coefficient (R)

The results indicate significant variations in the accuracy of predictions across the tested network architectures. Among the different ANN configurations, the 6-4-3-1 ANN architecture exhibited the best predictive performance, achieving the highest correlation coefficient (R = 0.966) and the lowest MPE (MPE = 4.3003%). These results validate the superior ability of this architecture to model the nonlinear relationship between the input variables and the temperature of the PV module accurately.

Additionally, this chosen 6-4-3-1 ANN model provides an optimal balance between network complexity and computational efficiency. The model successfully captures the complex nonlinear trends within the data without overfitting, ensuring that it generalizes well to unseen data. This capability makes it highly applicable for reliable performance predictions under various operational conditions, demonstrating that it can be effectively deployed for real-time performance forecasting and optimization of PV/T systems.

**Table 2.** Comparative performance of Artificial Neural Network (ANN) models

| Property | 6-3-1 | 6-5-1 | 6-4-3-1 | 6-5-4-3-1 |
|---|---|---|---|---|
| Convergence time (sec) | 12 | 23 | 24 | 27 |
| Train R (%) | 0.937 | 0.957 | 0.949 | 0.951 |
| Train MSE | 0.00195 | 0.00131 | 0.0013 | 0.00122 |
| Test R (%) | 0.947 | 0.957 | 0.966 | 0.951 |
| Test MBE | 0.1635 | 0.4750 | 0.5114 | 0.4392 |
| Test RMSE | 0.1126 | 0.1036 | 0.1009 | 0.1055 |
| Test MPE (%) | 4.90 | 4.74 | 4.3003 | 4.7301 |

Note: Mean Bias Error (MBE); Root Mean Square Error (RMSE); Mean Percentage Error (MPE).

The validity and reliability of the simulation model were verified by comparing the model's outputs to the corresponding experimental data. This comparison is crucial for evaluating the model's potential to accurately represent the physical behavior of the hybrid PV/T system under various operating conditions. Figure 20 presents a comparison of simultaneous daytime measurements of PHM-CT sensor data and ANN model predictions of the cell temperature over a typical daily period, from 8:00 AM to 6:00 PM. Both the experimental findings and the predicted values (represented by the fitting curve) are shown in the Figure 20, demonstrating that the two sets of data are in excellent agreement.

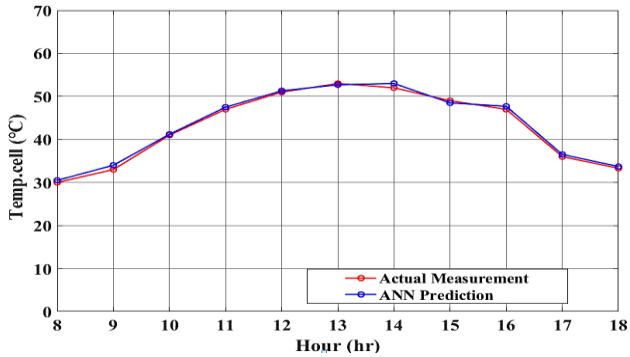


**Figure 20.** Comparison of actual and predicted temperature values

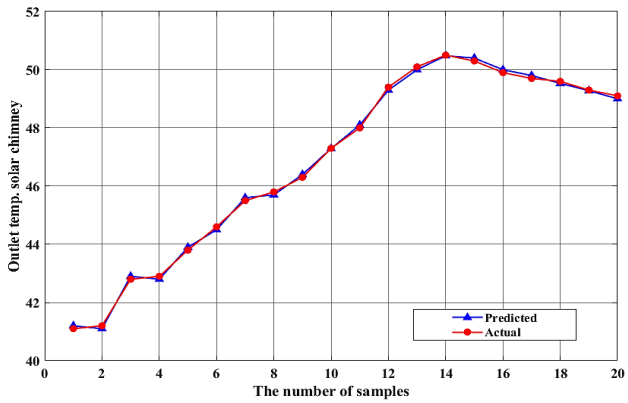


**Figure 21.** Actual and predicted outlet temperature of the solar chimney (SC)

The temperature of the PV module starts at 30 °C in the early morning and gradually increases as solar radiation intensifies. The maximum temperature of 52 °C is reached between 1:00 PM and 2:00 PM, coinciding with peak solar irradiance. At midday, the maximum difference between the predicted and observed temperatures is less than 1 °C, which indicates exceptional model accuracy under high solar radiation conditions. This suggests that the ANN model is highly effective at capturing the system's thermal behavior and accurately predicting the cell temperature even during rapid fluctuations in solar irradiance.

Furthermore, the ANN model accurately responds to sudden changes in cell temperature, demonstrating its capability to adapt to dynamic operating conditions. This strong agreement between the experimental data and the model predictions confirms the reliability of the model in predicting thermal performance under varying environmental factors, making it a robust tool for optimizing PV/T system performance.

Figure 21 shows the predicted and test outlet air temperatures of the SC over the amount of 20 test samples. The results show a good consistency of the ANN-predicted values with each of the actual measurements and that deviations within the full range of the sample are small, confirming good precision for the proposed model. The outlet air temperature shows a gradual increase from around 42 °C at the first sample up to its maximum of about 51 °C at the 15th sample. Below this level, there is relatively little cooling observed in succeeding samples. This trend reflects the solar insolation and ambient condition difference during measurements, and proves again the accuracy of ANN model to trace the dynamic thermal performance of SC.

5.3.2 Experimental and Artificial Neural Network model results for efficiency modeling

A systematic assessment of the predictive capabilities of the ANNs developed for predicting the thermal and electrical efficiencies of the PV/T system is presented in Table 3. The comparison highlights the performance of different network architectures and their ability to predict efficiency profiles under varying operating conditions. The analysis shows that different ANN structures perform differently depending on the operating modes, with certain designs offering better prediction accuracy for specific system behaviors.

**Table 3.** ANN structure performance in predicting PV/T efficiencies

| ANN Model | ANN Structure | Target | RMSE | $R^2$ | COV |
|---|---|---|---|---|---|
| 1 | 6-10-1 | $\eta_{th}$ | 0.3747 | 0.9951 | 0.0439 |
| | | $\eta_{ele}$ | 0.1344 | 0.9832 | 0.0133 |
| 2 | 6-20-1 | $\eta_{th}$ | 1.165 | 0.9775 | 0.1564 |
| | | $\eta_{ele}$ | 0.149 | 0.9741 | 0.01536 |
| 3 | 6-10-20-1 | $\eta_{th}$ | 0.569 | 0.9985 | 0.1189 |
| | | $\eta_{ele}$ | 0.8905 | 0.9439 | 0.0468 |

Note: Artificial Neural Network (ANN); Photovoltaic/thermal (PV/T); Root Mean Square Error (RMSE).

Among the tested models, the 6-10-1 ANN architecture delivered the most accurate predictions of thermal efficiency, with an impressive coefficient of determination ($R^2 = 0.9951$) and an RMSE = 0.3747. These performance metrics indicate that the 6-10-1 ANN model is highly reliable in predicting thermal efficiency, with only minimal deviations from the experimental data. The $R^2$ value close to 1 suggests that the model explains a very high proportion of the variability in thermal efficiency, while the low RMSE indicates that the predictions are highly consistent with the measured values.

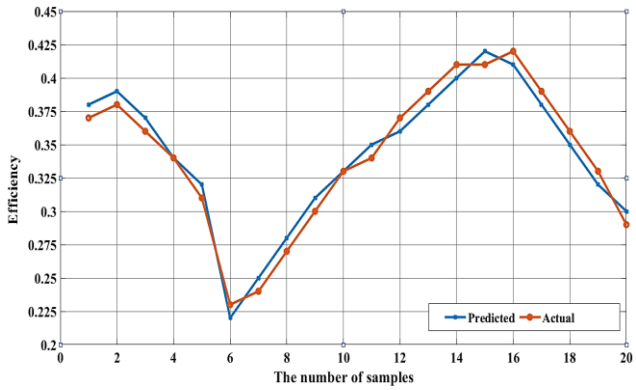


**Figure 22.** Comparison of the electrical efficiency

Figures 22 and 23 present a comparative analysis between the experimental and ANN-estimated thermal and electrical efficiencies of the PV/T system. The results indicate an excellent match between the actual and predicted values across all tested operating points, confirming that the proposed ANN model is highly accurate. The model's predictions closely follow the temporal patterns and degradations of both thermal and electrical efficiencies, capturing the system's behavior under both peak and off-peak performance conditions.

The small residuals observed between the experimental data and the predicted values further emphasize the high accuracy of the ANN model. These minor deviations highlight that the model is able to predict system performance with a high degree of reliability, demonstrating its ability to effectively model the complex and nonlinear relationships inherent in the behavior of the hybrid PV/T–SC system.

These findings validate the ANN model as a trustworthy tool for modeling and predicting the performance of PV/T systems. Given its ability to handle the nonlinear characteristics of the system and its strong agreement with experimental data, the ANN model can be employed as an efficient computational tool for performance prediction and analysis under varied climatic and operational conditions. The results further support the potential of using ANN-based models for optimizing system performance and guiding future PV/T system designs.

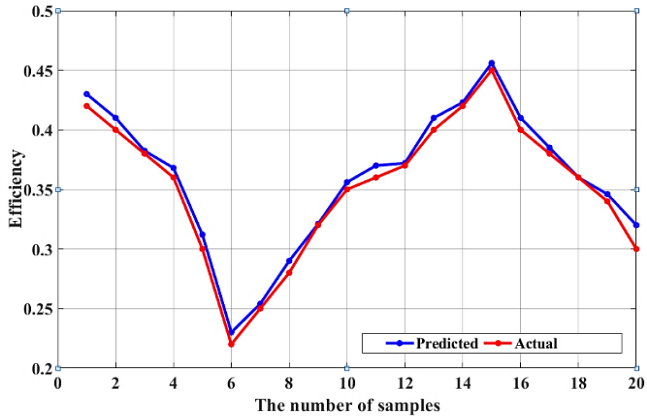


**Figure 23.** Comparison of the thermal efficiency

**Table 4.** Comparison of Artificial Neural Network (ANN) model predictions with traditional regression and theoretical models

| Aspect | ANN Model | Traditional Regression Models | Theoretical Models |
|---|---|---|---|
| Model Type | Data-driven, nonlinear model | Assumes linear relationships | Based on simplified assumptions and physical principles |
| Accuracy | High accuracy, handles complex and nonlinear behaviors | Moderate accuracy, struggles with nonlinearity | Provides qualitative insights, but less accurate for dynamic systems |
| Adaptability | Learns from real-world data, adapts to changes in conditions | Limited by the assumptions inherent in the regression model | Rigid assumptions, may not adapt well to dynamic conditions |
| Handling of Nonlinear Relationships | Excellent at capturing nonlinear interactions | Poor at capturing nonlinearities | Limited to linear approximations or simplified models |
| Real-World Data Integration | Trained on real-world data to improve prediction accuracy | Often fails to incorporate real-world data variability | Assumes idealized conditions, doesn't incorporate real-world variations |
| System Complexity | Handles complex systems with multiple variables | Struggles with complexity and interdependencies | Simplifies the system, omitting many real-world complexities |
| Efficiency in Dynamic Conditions | High performance under fluctuating conditions | Less accurate under fluctuating or extreme conditions | Struggles to predict accurately in dynamic conditions |
| Application | Suitable for dynamic, real-time performance predictions | Best for simpler systems or when relationships are linear | Suitable for basic understanding of system behavior but lacks precision in dynamic environments |

**Table 5.** Comparison of studies on photovoltaic/thermal (PV/T) systems and solar chimney (SC) optimization with Artificial Neural Network (ANN) integration

| Study Reference | Research Focus | Key Findings |
|---|---|---|
| Khaleel et al. [6] | Photovoltaic (PV) panel performance with hydraulic cooling. | 29.11% increase in daily electricity efficiency with hydraulic cooling. |
| Tiwari et al. [11] | Review of PV/T technology and performance evaluation. | Improved system efficiency in hybrid PV/T systems, with varying performance. |
| Bijjargi et al. [14] | Cooling techniques for PV modules. | 10-20% increase in efficiency depending on cooling method. |
| Jalil et al. [15] | Thermal performance of air solar collectors. | 3-inlet design resulted in higher exit temperatures, improving performance. |
| Oussama et al. [17] | Inclined solar chimneys for building ventilation. | Optimal design improved ventilation efficiency by 15-30%. |
| Abdeen et al. [19] | Solar chimney optimization in Egypt. | Enhanced thermal comfort during peak sun hours. |
| Present Study | Hybrid PV/T system with solar chimney, optimized using ANN. | Electrical efficiency improved from 13% to 15.8%, thermal efficiency ranged from 30% to 57%, with an $R^2$ of 0.9951 and Root Mean Square Error (RMSE) of 0.3747. PV Temperature reduced by up to 13 °C. |

5.3.3 Performance evaluation using key metrics

To evaluate the precision and strength of the ANN model, key performance indices were used, including the MBE, RMSE, and the correlation coefficient (R). These metrics, when applied to both thermal and electrical efficiency predictions, indicate that the model exhibits exceptional performance:

- Thermal Efficiency: The model achieved a correlation coefficient ($R^2$ = 0.9951), indicating that it explains over 99% of the variance in thermal efficiency. The RMSE (0.3747) further validates the model's accuracy by indicating minimal error in the predictions.
- Electrical Efficiency: The model's predictions were similarly accurate, with residuals showing a high degree of correlation between experimental and predicted values, demonstrating that the model consistently captures electrical performance under real conditions.

Table 4 shows the comparison between the ANN model predictions, traditional regression models, and theoretical models.

### 5.4 Comparison with previous studies

As the demand for sustainable energy solutions continues to grow, optimizing the performance of PV/T systems and SCs has become a key area of research. Various methods, including cooling techniques for PV panels and adjustments to SC configurations, have been explored to enhance system performance. Additionally, the integration of ANNs has shown promise in improving the electrical and thermal efficiency of these hybrid systems.

Table 5 provides a comparison of significant studies in this field, focusing on different approaches to optimizing PV/T systems and SCs. The table summarizes key findings from studies that examined hydraulic cooling methods, the impact of cooling techniques on conversion efficiency, and the optimization of SC design parameters. The table also highlights the results of the present study, which integrates an ANN-based optimization approach to improve both electrical and thermal performance of the hybrid PV/T system with a SC.

## 6. CONCLUSIONS

This study confirms the effectiveness of integrating a SC with a PV/T system and highlights the important role of AI, specifically ANNs, in enhancing system performance and predictive accuracy. The combined experimental investigation and ANN-based modelling approach demonstrates that coupling physical system optimization with intelligent data-driven techniques offers a promising pathway for the development of high-efficiency hybrid solar energy systems capable of simultaneously producing electrical and thermal energy.

**Key Contributions:**

- **Novel System Configuration:** This study introduces a hybrid PV/T system integrated with a SC, a novel configuration that allows for the simultaneous generation of both thermal and electrical energy, improving the overall system performance. The integration of the SC effectively reduces the temperature of the PV module, leading to an increase in electrical efficiency.
- **Multi-Objective Analysis**: A significant innovation in this work is the application of a performance index for system optimization. The developed method accurately evaluates the system's thermal and electrical performance, providing high analytical accuracy. This index-based approach offers reliable performance evaluation, allowing for efficient management of the system under varying operational conditions.
- **Optimization Principle:** The study emphasizes the optimization of airflow rates to improve thermal efficiency, a concept that has not been extensively explored in previous studies. By adjusting airflow, the system maximizes heat dissipation, leading to a significant improvement in thermal performance.

Based on the detailed experimental and analytical analysis, the following key conclusions can be drawn:

1) **Improved electrical performance:** The integration of the SC significantly reduced the operating temperature of the PV cells by approximately 5–13 °C compared to the uncooled condition. This reduction in cell temperature effectively minimized thermal losses and led to a noticeable enhancement in electrical efficiency, which increased from about 13% in the uncooled case to approximately 15.8% at the highest air mass flow rate. Consequently, a significant improvement in electrical power output was achieved.
2) **Enhanced thermal efficiency:** The thermal efficiency of the hybrid PV/T system ranged between 30% and 57%, depending on the airflow rate. At lower air mass flow rates, higher outlet temperature differences (up to 4.8 °C) were observed due to longer air residence time within the collector channel. Conversely, at higher airflow rates, the overall heat transfer rate increased, resulting in improved thermal efficiency. These findings indicate that the system can be effectively adapted to different operating conditions to maximize heat recovery performance.
3) **High prediction accuracy of ANN models:** The ANN models successfully captured the dynamic thermal and electrical behavior of the hybrid system, demonstrating low RMSE values for temperature prediction and an average deviation of less than 1 °C between predicted and experimental temperature values. Moreover, high correlation coefficients (R > 96%) and coefficients of determination ($R^2$ > 0.99) confirm the strong predictive capability of the developed ANN models for both PV module and SC outlet temperatures.
4) **Reliable estimation of system efficiencies:** The ANN-based efficiency prediction models exhibited high reliability for both electrical and thermal efficiencies, with $R^2$ values exceeding 0.98. These results demonstrate the ability of ANN techniques to accurately model the nonlinear and complex interactions governing the performance of hybrid PV/T–SC systems without overfitting or loss of generalization capability.
5) **Practical applicability and sustainability potential:** The AI-supported PV/T–SC hybrid system demonstrated strong practical feasibility for deployment in hot and arid regions. Its potential applications include solar-assisted cooling, air conditioning, agricultural drying and cooling, and enhanced electricity generation. The effective utilization of waste heat through the SC further contributes to improved energy efficiency and supports the development of more sustainable and resilient future energy systems.

## 7. LIMITATIONS OF THE STUDY

Even though the results of the latest study are valuable in determining the performance of the hybrid PV/T–SC system, there are some limitations that should be noted. Here are these restrictions:

- The current experiments were performed under summer-specific climatic conditions of Baghdad, which may restrict the generalization of results to other climates or seasons.
- The system was tested only within a limited air mass flow rate range, so the optimum operating conditions may not have been accessed.
- It relied on a single monocrystalline PV module and did not explore the impact of different PV technologies or module regimes.
- The ANN model was developed based on a small amount of data, and that might cause some errors in predicting for an untested operation range.
- The ANN model is data-based and doesn't consider the detailed operation mechanism of heat transfer and airflow in the system.
- Effects of long-term operations, including aging and dust accumulation, were not included in the analysis.

## 8. FUTURE DIRECTIONS

The study's results and limitations suggest a few avenues for future research:

- Studying the viewpoint of PV/T–SC component in different weather conditions and seasons to find out the feasibility and reliability of such systems in various places.
- Investigating a broader range of AMF and advanced air flow control ideas for better operation and higher electrical/thermal efficiency.
- Studying the effect of various PV technologies, module layouts, and absorber concepts on system performance and thermal response.
- Incorporating long-term performance analysis to determine the impact of dust accumulation, component degradation, and environmental degradation on system efficiency and durability.
- Further development of the ANN-based modelling scheme with larger input/output datasets, and introduction of hybrid models by fusing data-driven techniques and physics-based models to enhance prediction accuracy/accessibility.
- Exploring the synergy between the developed PV/T–SC system and application systems in practical including solar cooling, agricultural drying, and building energy system to improve its applicability and economic value in markets.

## REFERENCES


[1] Shang, Y., Hammoodi, K.A., Alizadeh, A.A., Sharma, K., Rajab, H., Ahmed, M., Kassim, M., Maleki, H., Salahshour, S. (2024). Artificial neural network hyperparameters optimization for predicting the thermal conductivity of MXene/graphene nanofluids. Journal of the Taiwan Institute of Chemical Engineers, 164: 105673. https://doi.org/10.1016/j.jtice.2024.105673

[2] Gautam, P., Kumar, S., Lokhandwala, S. (2019). Energy-aware intelligence in megacities. Current Developments in Biotechnology and Bioengineering, Elsevier, pp. 211-238. https://doi.org/10.1016/B978-0-444-64083-3.00011-7

[3] Jadallah, A.A., Alsaadi, M.K., Hussien, S.A. (2020). The hybrid (PVT) double-pass system with a mixed-mode solar dryer for drying banana. Engineering and Technology Journal, 38(8): 1214-1225.

[4] Khalaf, A.F., Basem, A., Hussein, H.Q., Jasim, A.K., Hammoodi, K.A., Al-Tajer, A.M., Omer, I., Flayyih, M.A. (2022). Improvement of heat transfer by using porous media, nanofluid, and fins: A review. International Journal of Heat and Technology, 40(2): 497-521. https://doi.org/10.18280/ijht.400218

[5] Rashid, F.L., Alkhekany, Z.A.K., Eleiwi, M.A., Bouabidi, A., Ahmad, S., Chibani, A., Kezzar, M., Kadhim, S.A., Askar, A.H., Hammoodi, K.A. (2025). A comprehensive review on natural convection in trapezoidal cavities with mono and hybrid nanofluids. International Journal of Thermofluids, 27: 101226. https://doi.org/10.1016/j.ijft.2025.101226

[6] Khaleel, F., Hasan, I., Mohammed, M. (2022). Control of PV panel system temperature using PID cuckoo search. Engineering and Technology Journal, 40(1): 249-256. https://etj.uotechnology.edu.iq/journal/vol40/iss1/29/.

[7] Abdulmunem, A.R., Samin, P.M., Rahman, H.A., Hussien, H.A., Mazali, I.I. (2020). Enhancing PV cells' electrical efficiency using phase change material with copper foam matrix and multi-walled carbon nanotubes as passive cooling method. Renewable Energy, 160: 663-675. https://doi.org/10.1016/j.renene.2020.07.037

[8] Shaeli, M., Baccar, M., Jalil, J. (2024). Solar photovoltaic thermal cells performance improvement using jet, phase change material and nanoparticles cooling technology: A review. Engineering and Technology Journal, 42(1): 51-64. https://etj.researchcommons.org/journal/vol42/iss1/4/.

[9] Abdulghafor, I.A., Ali, S.A., Kadhim, S.A., Al-Mrayatee, H.M., Hammoodi, K.A. (2024). Exergy analysis of a solar heating system in indoor spaces. International Journal of Heat and Technology, 42(5): 1551-1558. https://doi.org/10.18280/ijht.420508

[10] Murtadha, T.K. (2023). Effect of using $Al_2O_3/TiO_2$ hybrid nanofluids on improving the photovoltaic performance. Case Studies in Thermal Engineering, 47: 103112. https://doi.org/10.1016/j.csite.2023.103112

[11] Tiwari, A.K., Chatterjee, K., Agrawal, S., Singh, G.K. (2023). A comprehensive review of photovoltaic-thermal (PVT) technology: Performance evaluation and contemporary development. Energy Reports, 10: 2655-2679. https://doi.org/10.1016/j.egyr.2023.09.043

[12] Sainthiya, H., Beniwal, N.S. (2020). Comparative analysis of electrical performance parameters under combined water cooling technique of photovoltaic module: An experimental investigation. Energy Sources, Part A: Recovery, Utilization, and Environmental Effects, 42(15): 1902-1913. https://doi.org/10.1080/15567036.2019.1604894

[13] Ghani, F., Rosengarten, G., Duke, M., Carson, J.K. (2015). On the influence of temperature on crystalline

silicon solar cell characterisation parameters. Solar Energy, 112: 437-445. https://doi.org/10.1016/j.solener.2014.12.018
[14] Bijjargi, Y.S., Kale, S.S., Shaikh, K.A. (2016). Cooling techniques for photovoltaic module for improving its conversion efficiency: A review. International Journal of Mechanical Engineering and Technology, 7(4): 22-38.
[15] Jalil, J.M., Ayaal, A.H., Hardan, A.A. (2020). Numerical investigation of thermal performance for air solar collector with multi inlets. IOP Conference Series: Materials Science and Engineering, 765(1): 012036. https://doi.org/10.1088/1757-899X/765/1/012036
[16] Elminshawy, N.A., El Ghandour, M., Gad, H.M., El-Damhogi, D.G., El-Nahhas, K., Addas, M.F. (2019). The performance of a buried heat exchanger system for PV panel cooling under elevated air temperatures. Geothermics, 82: 7-15. https://doi.org/10.1016/j.geothermics.2019.05.012
[17] Oussama, B., Abdelmadjid, D., Noureddine, H., Slimani, M.E.A., Abdessamia, H. (2025). An experimental investigation of an inclined solar chimney integrated into residential buildings with different materials construction for natural ventilation in a hot-arid climate. Journal of Thermal Engineering, 11(3): 643-658. https://doi.org/10.14744/thermal.0000936
[18] Natarajan, R., Suni, A.C.K., Pedasingu, L.R., Sampath, Y. (2021). Numerical and experimental study on the collector and chimney modifications of a solar chimney power plant. Journal of Thermal Engineering, 10(6): 1539-1558. https://doi.org/10.14744/thermal.0000887
[19] Abdeen, A., Serageldin, A.A., Ibrahim, M.G., El-Zafarany, A., Ookawara, S., Murata, R. (2019). Solar chimney optimization for enhancing thermal comfort in Egypt: An experimental and numerical study. Solar Energy, 180: 524-536. https://doi.org/10.1016/j.solener.2019.01.063
[20] Attia, H., Hossin, K., Al Hazza, M. (2023). Experimental investigation of photovoltaic systems for performance improvement using water cooling. Clean Energy, 7(4): 721-733. https://doi.org/10.1093/ce/zkad03
[21] Natsheh, E.M. (2013). Hybrid power systems energy management based on Artificial Intelligence. Doctoral Dissertation. Manchester Metropolitan University. https://e-space.mmu.ac.uk/id/eprint/314015.
[22] Jarimi, H., Bakar, M.N.A., Othman, M., Din, M.H. (2016). Bi-fluid photovoltaic/thermal (PV/T) solar collector: Experimental validation of a 2-D theoretical model. Renewable Energy, 85: 1052-1067. https://doi.org/10.1016/j.renene.2015.07.014
[23] Naqvi, A.A., Ahmed, A., Jamal, M., Majeed, A., Khizar, A., Shaheer, B. (2022). Performance evaluation of hybrid PVT air collector. A comparative approach. GMSARN International Journal, 16(2): 121-127.
[24] El Manssouri, O., El Fouas, C., Hajji, B., Rabhi, A., Tina, G.M., Gagliano, A. (2020). Modeling and performances assessments of PV/T bifluid hybrid collector: Three cooling modes operation case. In 2020 International Conference on Electrical and Information Technologies (ICEIT), Rabat, Morocco, pp. 1-6. https://doi.org/10.1109/ICEIT48248.2020.9113233
[25] Hussain, F., Othman, M.Y.H., Yatim, B., Ruslan, H., Sopian, K., Ibarahim, Z. (2013). A study of PV/T collector with honeycomb heat exchanger. AIP Conference Proceedings, 1571(1): 10-16. https://doi.org/10.1063/1.4858622
[26] Serbouti, A., Rattal, M., Boulal, A., Oualim, E.M., Mouhsen, A. (2018). Technical & economical assessment of a hybrid PV thermal system in Morocco. AIP Conference Proceedings, 2056(1): 020002. https://doi.org/10.1063/1.5084975
[27] Abdulmajeed, O.M., Jadallah, A.A., Bilal, G.A., Arıcı, M. (2022). Experimental investigation on the performance of an advanced bi-fluid photovoltaic thermal solar collector system. Sustainable Energy Technologies and Assessments, 54: 102865. https://doi.org/10.1016/j.seta.2022.102865
[28] Dorvlo, A.S., Jervase, J.A., Al-Lawati, A. (2002). Solar radiation estimation using artificial neural networks. Applied Energy, 71(4): 307-319. https://doi.org/10.1016/S0306-2619(02)00016-8
[29] Negnevitsky, M. (2011). Artificial Intelligence 3e e-book. A guide to intelligent systems. Artificial Intelligence, 73(1-2).
[30] Trifonov, R., Yoshinov, R., Pavlova, G., Tsochev, G. (2017). Artificial neural network intelligent method for prediction. AIP Conference Proceedings, 1872(1): 020021. https://doi.org/10.1063/1.4996678